Journal of Photochemistry and Photobiology A: Chemistry 288 (2014) 60–69

Contents lists available at ScienceDirect

Journal of Photochemistry and Photobiology A: Chemistry

journal homepage: www.elsevier.com/locate/jphotochem

Light initiated *E–Z* and *Z–E* isomerization of isatinphenylsemicarbazones: Tautomeric equilibrium effect

Klaudia Jakusová [a], Marek Cigáň [a,*], Jana Donovalová [a], Martin Gáplovský [b], Robert Sokolík [a], Anton Gáplovský [a]

[a] Faculty of Natural Sciences, Institute of Chemistry, Comenius University, Mlynská dolina CH-2, SK-842 15 Bratislava, Slovakia
[b] Department of Pharmaceutical Chemistry, Faculty of Pharmacy, Comenius University, Odbojárov 10, SK-832 32 Bratislava, Slovakia

ARTICLE INFO

Article history:
Received 7 February 2014
Received in revised form 7 May 2014
Accepted 10 May 2014
Available online 16 May 2014

Keywords:
Isatinphenylsemicarbazones
Light initiated *E–Z* and *Z–E* isomerization
Thermally initiated back reaction
Tautomeric equilibrium effect

ABSTRACT

The light and thermally initiated mutual *E*- and *Z*-isomer transformations of two efficient isatin *N*-phenylsemicarbazone colorimetric sensors for strongly basic anions differing in sensitivity, selectivity and sensing mechanism were investigated in solvents of different polarity. The reaction mechanism of photochemically and thermally initiated *E–Z* isomerization and the absence of back *Z–E* isomerization is discussed in terms of self-aggregate formation, hydrazide-hydrazonol tautomeric equilibrium, the role of intra- and inter-molecular hydrogen bonds, excited-state proton transfer, solvent polarity and concentration effects. The effect of the activation energies related to conformational and geometric changes of the isomers and the possible analytical application were investigated. Theoretically calculated properties are in good agreement with obtained experimental results and support the proposed reaction mechanism.

1. Introduction

E–Z isomerization of organic compounds, including C=C, C=N or N=N double bond isomerization, is among the most studied photochemical and thermal reactions and thus continues to attract scientific attention. Research in this area now focuses on practical applications of *E–Z* isomerization, particularly in the field of organic electronics. Due to the photochromic properties of organic compounds containing C=C, C=N or N=N double bonds, photoinitiated *E–Z* isomerization reaction mechanism is a powerful tool in the development of photo-optical switches and optical memories [1–7].

Reaction pathway control is essential for practical application of *E–Z* isomerization. Therein, the study of reaction mechanism, kinetics, structure–property and structure–environment relationships, and the subsequent active control of *E–Z* isomerization play key roles. For example, conformational or spatial *E–Z* isomerization restriction of the C=N bond, due to sensor–metal cation interaction was used in the design of new metal cation sensing mechanisms to provide simple and efficient fluorescence enhancement [8].

This advance was based on previous studies investigating external stimuli influence on receptor conformer populations. Wu et al. established that *E–Z* isomerization effectively competed with radiation deactivation of excited molecules leading to rapid fluorescence quenching [9].

Other types of "host–guest" intermolecular interactions can also influence *E–Z* isomerization efficiency (quantum yield) or the overall ratio of potential isomers. Signal molecules thus obtain properties of a sensor (receptor). In that manner, the photoisomerization of azobenzenes, stilbenes, spiropyrans and rhodopsine was used for enzyme activity monitoring [10–12].

Supramolecular chemistry has focused on the development of selective colorimetric or fluorescent anion sensors for the last twenty years [13–16], and researches including Wenzel, Chudzinski, Bergamaschi, Jiménez, Martínez-Máñez and Gale continue this work [17–22].

Anion induced tautomerism of isatin-3-4-phenyl(semicarbazone) derivatives was investigated in our recent study (Scheme 1) [23]. The interaction of F^-, AcO^-, $H_2PO_4^-$, Br^- or HSO_4^- anions with *E*- and *Z*-isomers of isatin-3-4-phenyl(semicarbazone) ***I*** and *N*-methylisatin-3-4-phenyl(semicarbazone) ***II*** as sensors influenced the equilibrium ratio of the individual sensor tautomeric forms in the liquid phase.

The *E*- and *Z*-sensor isomers differed in sensitivity, selectivity and sensing mechanism. The equilibrium ratio of the individual tautomeric forms, affected by (1) the inter- and intra-molecular interaction modulation of isatinphenylsemicarbazone molecules

* Corresponding author. Tel.: +421 2 60296306; fax: +421 2 60296342.
E-mail addresses: jakusova@fns.uniba.sk (K. Jakusová), cigan@fns.uniba.sk (M. Cigáň), donovalova@fns.uniba.sk (J. Donovalová), gaplovsky@fpharm.uniba.sk (M. Gáplovský), sokolik@fns.uniba.sk (R. Sokolík), gaplovsky@fns.uniba.sk (A. Gáplovský).

http://dx.doi.org/10.1016/j.jphotochem.2014.05.004
1010-6030/

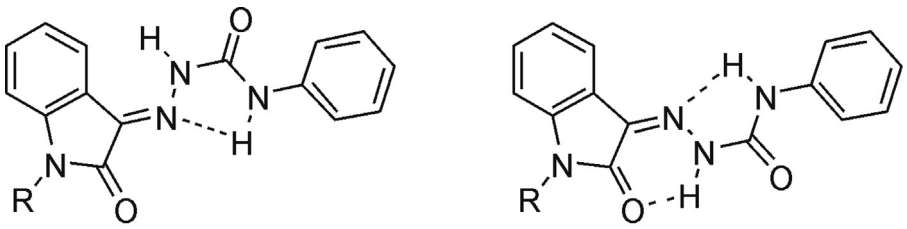

E-isomers:		*Z*-isomers:	
R = H	***Ia***	R = H	***Ib***
R = CH_3	***IIa***	R = CH_3	***IIb***

Scheme 1. Molecular structure of the studied isatinphenylsemicarbazones.

by anion induced change in receptor molecule solvation shells and (2) the sensor–anion interaction with urea hydrogens, was easily determined by UV–vis spectroscopy. The appropriate selection of experimental conditions led to a high degree of sensor selectivity for some investigated anions. Sensors ***Ia***–***IIb*** provided an excellent signal to noise ratio and also a wide detection range. Detection of F^- or CH_3COO^- anions at high weakly-basic anion excess was also possible. Furthermore, due to excellent *E*-isomer sensitivity in organic media, these isomers can be used for F^- or CH_3COO^- sensing in semi-aqueous media.

Our quoted study [24] showed that the aggregate formation in weakly interacting non-polar solvents at higher isatinphenylsemicarbazone ***Ia*** and ***IIa*** concentrations prevents their room temperature *E*–*Z* isomerization to more stable *Z*-isomers. In contrast to the situation in non-polar solvents, *E*–*Z* isomerization from the monomeric form of phenylsemicarbazone *E*-isomers ***Ia*** and ***IIa*** occurs in highly interactive polar solvents only at temperatures above 70 °C. The aggregate formation at higher ***Ia*** and ***IIa*** concentrations and the presence of a new hydrazonol tautomeric form with a high degree of conjugation at low ***Ia*** and ***IIa*** concentrations prevent the room temperature *E*–*Z* isomerization of ***Ia*** and ***IIa*** in highly interactive polar solvents. In addition, no formation of the corresponding *E*-isomers was observed during thermally initiated back *Z*–*E* isomerization.

Herein, the tautomeric equilibrium effect on light initiated *E*–*Z* isomerization quantum yield of isatinphenylsemicarbazones ***I*** and ***II*** is reported; including comprehensive investigation of the thermally initiated back *Z*–*E* isomerization. This research is necessary for practical application of these compounds as anion sensors and also for better understanding of the photophysical properties of their subsequent derivatives for effective development and design of novel anion sensors. This investigation can also be useful in evaluation of the applicability of this type of compounds in chemical actinometry or molecular switching.

2. Experimental and theoretical methods

2.1. Synthesis

Synthesis of the studied compounds was published by Jakusová et al. [25].

2.2. Spectroscopic measurements

Electronic absorption spectra were obtained on a HP 8452A (Hewlett Packard, USA) diode array spectrophotometer, and fluorescence measurements were performed by the FSP 920 (Edinburgh Instruments, UK) spectrofluorimeter. The dimethylformamide (DMF), methanol (MeOH), acetonitrile (MeCN), benzene and dichloromethane (CH_2Cl_2) were all UV-spectroscopy or HPLC grade (Merck, Darmstadt, Germany; Fisher Slovakia, Levoča, Slovakia). All photochemical measurements were performed at 25 °C in the dark, with only 405 nm (or 341 nm) LED diodes Thorlabs as light sources with optical power of $P = 6$ mW and $P = 0.33$ mW, respectively.

2.3. Light initiated E–Z and Z–E isomerization

2.3.1. General procedure

Photochemical measurements were performed using the apparatus described elsewhere (Fig. 7 in [26] – without ultrasonic horn H and lens L_1; using Ocean Optics SD 2000 diode array spectrophotometer). The light sources were four 405 nm LED diodes Thorlabs with overall incident photon flux $I_0 = 5.6 \pm 0.1 \times 10^{-4}$ mol s^{-1} dm^{-3}, or three 341 nm LED diodes Thorlabs. The actual concentration of compounds studied in air-saturated solutions during irradiation in a 1 cm quartz fluorescence cuvette was measured spectrophotometrically in right-angle arrangement (HP 8452A). The LED light sources were turned off during the concentration measurements. The incident concentrations of the studied isomer were $c_0 = 1 \times 10^{-4}$ mol dm^{-3} and 3×10^{-6} mol dm^{-3}. The presence of the second isomer during the irradiation of the corresponding *E*- or *Z*-isomer was confirmed/negated by HPLC chromatography, as described in Section 2.4.1.

2.3.2. Quantum yield determination

The *E*–*Z* isomerization quantum yield (Φ_{E-Z}) of isatinphenylsemicarbazone *E*-isomers ***Ia*** and ***IIa*** in solution was determined according to Eqs. (1) and (2):

$$\Phi_{E-Z} = \frac{\int_{c_0}^{c_t} dc}{\int_0^t I_a dt} = \frac{\Delta c}{\int_0^t I_a dt} \quad (1)$$

$$\Delta c = \frac{\Delta A_\lambda}{\varepsilon_{\lambda Z} - \varepsilon_{\lambda E}} \quad (2)$$

where Δc is the concentration change in *E*- or *Z*-isomer, I_a is the absorbed photon flux by *E*-isomer at the irradiation wavelength λ using a monochromatic light source, ΔA_λ is the absorbance change at irradiation wavelength λ using a monochromatic light source, $\varepsilon_{\lambda E}$ is the molar extinction coefficient of *E*-isomer at irradiation wavelength λ using a monochromatic light source, $\varepsilon_{\lambda Z}$ is the molar

extinction coefficient of *Z*-isomer at irradiation wavelength λ using a monochromatic light source and *t* is irradiation time.

The *E*-isomer absorbed photon flux I_a at particular irradiation times during *E*–*Z* isomerization at irradiation wavelength λ = 405 nm and incident *E*-isomer concentration c_0 was calculated by Eq. (3) [27]:

$$I_{a,405E} = I_0 \frac{\varepsilon_{E,405}(c_0 - \Delta c)}{\varepsilon_{E,405}(c_0 - \Delta c) + \varepsilon_{E,405}\Delta c} \times [1 - 10^{-[\varepsilon_{E,405}(c_0-\Delta c)+\varepsilon_{E,405}\Delta c]}] \quad (3)$$

In the case of photochemically initiated *Z*-isomer degradation appearance during ***Ib*** (or ***IIb***) solution irradiation at 405 nm, the values of parameters Δc and I_a were estimated as the initial values at low *E*–*Z* isomerization conversion. Here, the rate of the competitive photochemical degradation was always less than the rate of ***Ia*** and ***IIa*** light initiated *Z*-isomer degradation.

The incident photon flux I_0 was determined by 2-nitrobenzaldehyde (2-NB) as chemical actinometer, according to Eq. (4) [28]:

$$I_0 = \frac{k}{2.303 \log \varepsilon_{2\text{-NB},405} \cdot \Phi_{2\text{-NB},405} \cdot l} \quad (4)$$

where $\varepsilon_{2\text{-NB},405}$ is the molar extinction coefficient of 2-NB at irradiation wavelength 405 nm, $\Phi_{2\text{-NB},405}$ is the quantum yield of 2-NB photodegradation at irradiation wavelength, *l* is the path length and *k* is the slope of the 2-NB first-order photodegradation plot under low-light-absorbing conditions (Fig. S1):

$$\ln\left(\frac{[2\text{-NB}]_t}{[2\text{-NB}]_0}\right) = -kt \quad (5)$$

2.4. Thermally initiated E–Z and Z–E isomerization

2.4.1. General procedure

Ten volumetric flasks with the particular *E*- or *Z*-isomer solution were thermostated at the corresponding temperature in a Julabo HE thermostat oil bath (Fisher Scientific, Czech Republic). One volumetric flask was removed form the oil bath at selected time intervals, cooled to 25 °C room temperature and analyzed by HPLC chromatography.

HPLC chromatography was performed using the Agilent Technologies chromatographic system. This consisted of 1100 series quarternary pump, column compartment, diode array detector (VWDG1314A) and manual injector (Rheodyne model 7725i) with 20 μM sample loop and degasser (g1379A). Column ZORBAX-SB-Phenyl (150 mm × 4.6 mm I.D.) was used in all experiments. Methanol was the mobile phase in analyses of the unmethylated semicarbazone ***I*** isomerization. For analyses of methylated semicarbazone ***II*** isomerization, mobile phase A was methanol (Merck, Lichrosolv) and phase B acetonitrile (Merck, Lichrosolv). Analysis of the reaction mixture: isocratic (for ***II*** isomerization, the ratio *A*/*B* was 1:1), instituted at 0.8 mL/min flow rate at 25 °C, with detection at 236 nm. The injection volume was 20 μL.

2.4.2. Theoretical calculations

The relative stabilities of isatin-phenylsemicarbazone isomers were investigated using quantum-chemical calculations. Structural geometries were optimized at the B3LYP 6-31+G(dp) level. Stationary points were characterized as minima by computations of harmonic vibration frequencies at the same theoretical level as the geometric optimization. Single point energies were calculated at the MP2 6-311++G(d,p) level. Zero-point vibration energies and thermal corrections to free energies were determined using unscaled B3LYP 6-31+G(dp) frequencies. All calculations were performed by the Gaussian 09 program package [29].

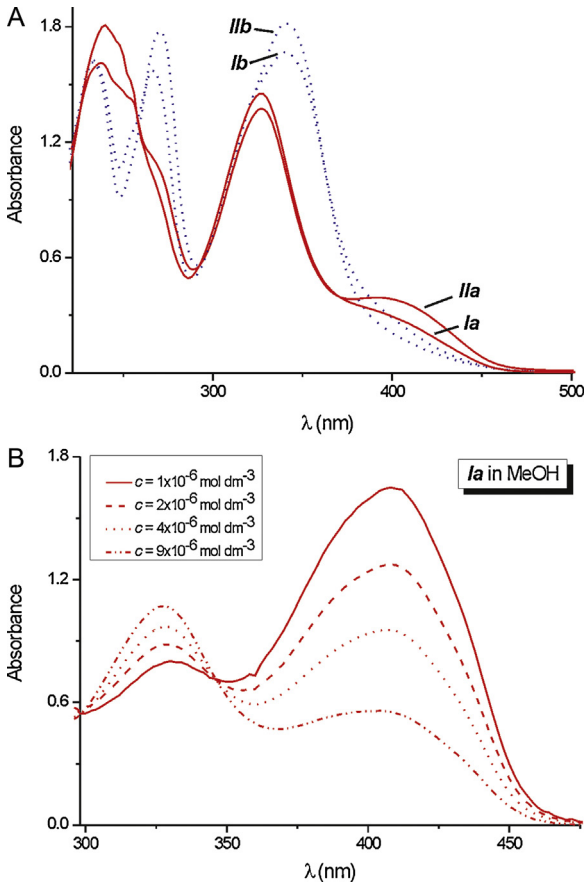

Fig. 1. (A) UV–vis spectra of *E*- and *Z*-isomers ***I*** and ***II*** in MeOH ($c = 10^{-4}$ mol dm^{-3}; $T = 25$ °C) and (B) dependence of UV–vis absorption spectra of ***Ia*** in MeOH on the ***Ia*** concentration ($T = 25$ °C).

3. Results and discussion

As described in our previous papers [24,25], the polarity of the solvent and concentration of isatin-3-4-phenyl(semicarbazones) ***I*** and ***II*** have a major impact on their UV–vis spectra. Depending on isatin-3-4-phenyl(semicarbazones) concentration, the UV–vis spectra of the *E*-isomers ***Ia*** and ***IIa*** in strongly interacting polar solvents have one or two main absorption maxima (λ_A) at approximately 330 nm and 410 nm (Fig. 1).

The presence of the absorption band at 410 nm for both *E*-isomers ***Ia*** and ***IIa***, and its increased intensity with decreasing concentration of these isomers, is explained by the existence of the hydrazide–hydrazonol chemical equilibrium (Scheme 2).

A decrease in concentration of *E*-isomers shifts the tautomeric hydrazide–hydrazonol equilibrium to the right, resulting in decreased associate formation. An increase in intensity of the hydrazonol C absorption band at 410 nm in strongly interacting polar solvents is accompanied by a decrease in the intensity of the absorption band for hydrazide B (and aggregate A) at approximately 330 nm. Compared to the hydrazide B form, the aggregate A form has almost the same shape, intensity and position of absorption maximum at approximately 330 nm. In weakly interacting solvents, such as benzene, $CHCl_3$ and MeCN, phenylsemicarbazone concentrations above 1×10^{-5} mol dm^{-3} again result in formation of dimers or higher aggregates of *E*-isomers ***Ia*** and ***IIa***. However, as expected, this occurs without the formation of hydrazonol C.

Due to existing intra-molecular hydrogen bonding, the corresponding *Z*-isomers ***Ib*** and ***IIb*** have only one bathochromically shifted λ_A at approximately 340 nm, and the longwavelength

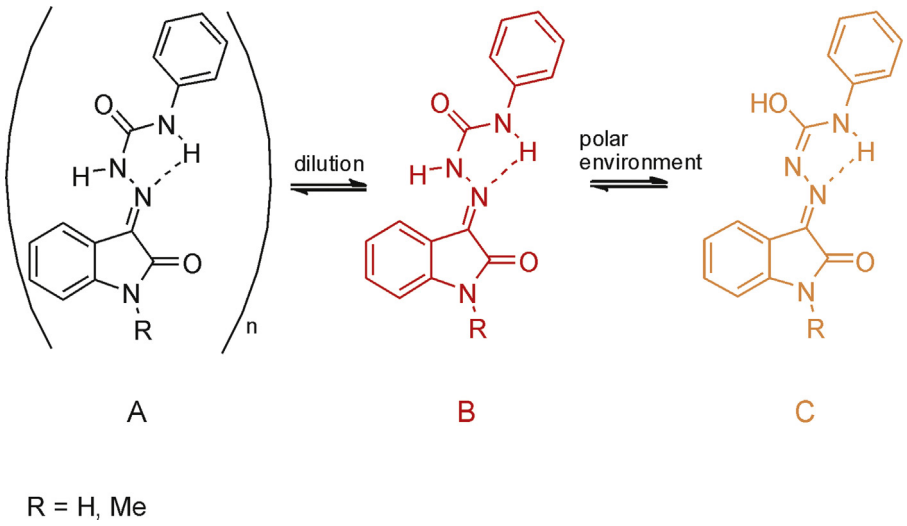

Scheme 2. Aggregate A/hydrazide B/hydrazonol C chemical equilibrium of the studied isatinphenylsemicarbazones.

absorption band at 410 nm was not observed in their UV–vis spectra in strongly interacting polar solvents.

3.1. Light initiated E–Z isomerization

To avoid Φ_{E-Z} distortion due to possible back *Z*–*E* photoisomerization (*Z*-isomers have higher molar extinctions in the long-wavelength absorption range of 320–380 nm – Fig. 1A [25]), and also molecule degradation using short-wavelength irradiation ($\lambda_{irr} < 320$ nm), 405 nm was chosen as the irradiation wavelength. At this wavelength, molar extinction coefficients of *E*-isomers are higher than for *Z*-isomers in strongly interacting polar solvents, and comparable to them in weakly interacting solvents (Figs. 1A and 2).

Furthermore, the hydrazonol tautomeric form with λ_A at 410 nm in strongly interacting polar solvents is responsible for the dominant absorption of *E*-isomers at low isatin-3-4-phenyl(semicarbazone) concentration (Figs. 1B and 3), thus allowing us to estimate the role of hydrazonol in light initiated *E*–*Z* isomerization of the studied compounds.

Both *E*-isomers quite rapidly isomerize to the corresponding *Z*-isomers under these experimental conditions (Figs. 4 and 5).

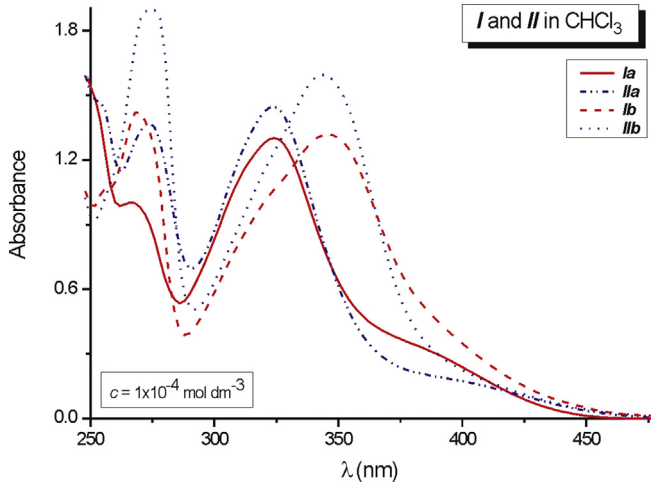

Fig. 2. UV–vis spectra of *E*- and *Z*-isomers ***I*** and ***II*** in $CHCl_3$ ($c = 10^{-4}$ mol dm^{-3}; $T = 25$ °C).

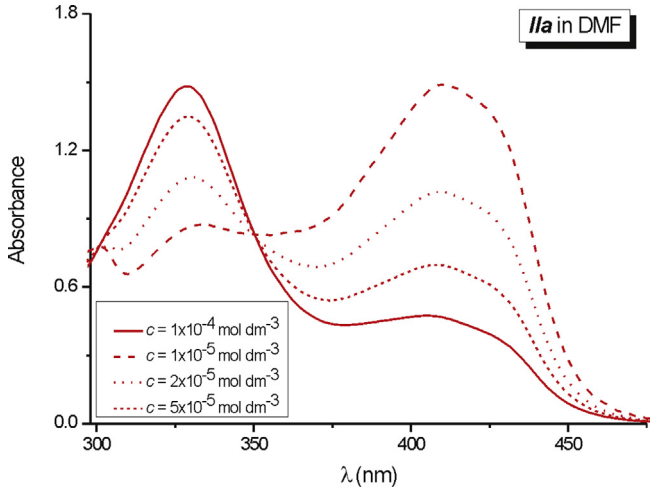

Fig. 3. Dependence of UV–vis absorption spectra of ***IIa*** in DMF on the ***IIa*** concentration ($T = 25$ °C).

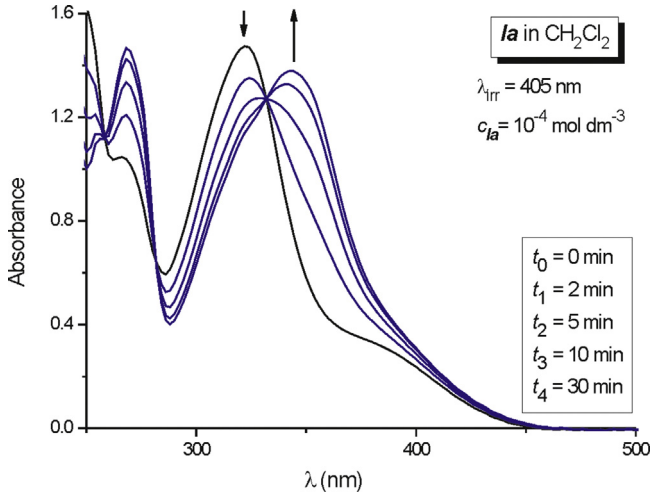

Fig. 4. Kinetic changes in the absorption spectra of ***Ia*** in CH_2Cl_2 during irradiation of ***Ia*** at 405 nm ($c_{Ia} = 1 \times 10^{-4}$ mol dm^{-3}; $I_0 = 5.6 \pm 0.1 \times 10^{-4}$ mol s^{-1} dm^{-3}).

Table 1
The *E–Z* isomerization quantum yield for isatinphenylsemicarbazone ***Ia*** in various solvents.

c [mol dm^{-3}]	Φ_{E-Z} (***Ia***) $\times 10^{-3}$				
	DMF	MeOH	MeCN	Benzene	CH_2Cl_2
1×10^{-4}	6.96 ± 0.13	3.20 ± 0.10	–[a]	3.93 ± 0.52	1.53 ± 0.12
3×10^{-6}	3.77 ± 0.18	2.55 ± 0.37	0.37 ± 0.05	2.48 ± 0.45	0.66 ± 0.08

Φ_{E-Z} – the *E–Z* isomerization quantum yield.
[a] Not soluble at this concentration.

Table 2
The *E–Z* isomerization quantum yield for isatinphenylsemicarbazone ***IIa*** in various solvents.

c [mol dm^{-3}]	Φ_{E-Z} (***IIa***) $\times 10^{-3}$				
	DMF	MeOH	MeCN	Benzene	CH_2Cl_2
1×10^{-4}	7.97 ± 0.39	4.43 ± 0.01	0.16 ± 0.05	0.36 ± 0.04	0.24 ± 0.05
3×10^{-6}	4.61 ± 1.80	1.34 ± 0.15	0.07 ± 0.06	0.13 ± 0.02	0.10 ± 0.03

Φ_{E-Z} – the *E–Z* isomerization quantum yield.

The *E–Z* isomerization quantum yield (Φ_{E-Z}) depends on solvent type, *E*-isomer concentration and the presence/absence of the $-CH_3$ substituent in position 1 of the isatin skeleton (Tables 1 and 2).

Tables 1 and 2 illustrate that the highest Φ_{E-Z} for these compounds at both 1×10^{-4} mol dm^{-3} and 3×10^{-6} mol dm^{-3} concentrations was in DMF. Depending on solvent type, the Φ_{E-Z} value for isatinphenylsemicarbazone *E*-isomer ***Ia*** decreases at the higher 1×10^{-4} mol dm^{-3} concentration in the following order: DMF > benzene > MeOH > CH_2Cl_2 > MeCN. It should be noted that Φ_{E-Z} is one magnitude higher in DMF, benzene and MeOH compared to CH_2Cl_2 and MeCN.

The decrease in concentration of both isatinphenylsemicarbazones ***Ia*** and ***IIa*** to 3×10^{-6} mol dm^{-3} leads to a 2- or 3-fold decrease in *E–Z* isomerization quantum yield in all solvents. At this low concentration, the Φ_{E-Z} of ***Ia*** decreases in the following order: DMF > benzene ~ MeOH > CH_2Cl_2 > MeCN. Almost the same Φ_{E-Z} decreased order at both low and high concentration was observed for *E*-isomer ***IIa***; with benzene providing the only exception.

These Φ_{E-Z} orders for both *E*-isomers illustrate the complex effects of solvents on Φ_{E-Z}. In the ground electronic state, the extent of the solvent's solvation capacity can stabilize or destabilize self-association of isatinpehnylsemicarbazone *E*-isomers and determine the hydrazide/hydrazonol ratio in solution (Scheme 2). In the excited state, solvent affects the energy and the competitive deactivation pathways of this state. In contrast to the other solvents used, MeOH and DMF have the highest Gutmann donor and acceptor numbers [30] and therefore effectively interact with hydrogen donor or acceptor parts of molecules ***Ia*** and ***IIa*** in their ground electronic state. These interactions can weaken the competitive intermolecular hydrogen bonding responsible for self-association of ***Ia*** and ***IIa*** (Scheme 2 – form A), resulting in dissociation of self-aggregates and an altered associate/hydrazide/hydrazonol ratio in solution. Tables 1 and 2 show that the Φ_{E-Z} values for ***Ia*** and ***IIa*** in the remaining three solvents do not correlate with Gutmann acceptor and donor values.

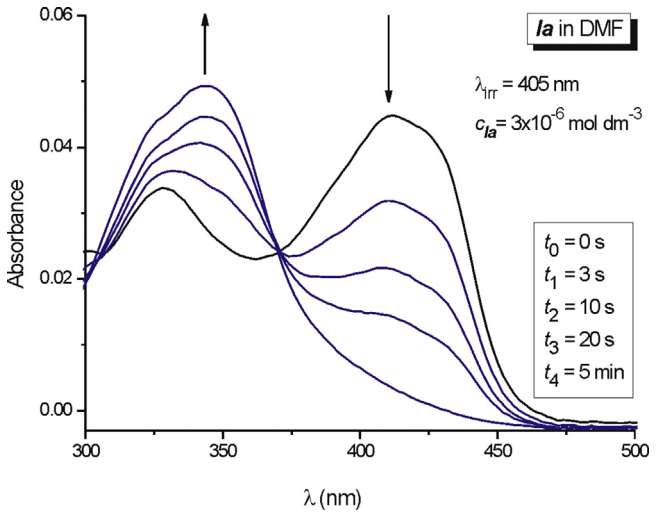

Fig. 5. Kinetic changes in the absorption spectra of ***Ia*** in DMF during irradiation of ***Ia*** at 405 nm ($c_{Ia} = 3 \times 10^{-6}$ mol dm^{-3}; $I_0 = 5.6 \pm 0.1 \times 10^{-4}$ mol s^{-1} dm^{-3}).

Although strongly interacting polar solvents reduce the intermolecular hydrogen bonding in the ***Ia*** and ***IIa*** aggregates, increased aggregate formation with increasing isatinphenylsemicarbazone concentration is evident in ^{1}H NMR and UV–vis spectroscopy measurements [24,25]. The concentration dependent shifts in emission maxima support aggregate formation in both strongly interacting polar solvents and weakly interacting ones – Figs. S2 and S3. We consider that dependence of the emission maxima on the excitation wavelength is associated with the different level and type of the formed ***Ia*** or ***IIa*** aggregates.

DMF and MeOH solvents have a high ability to interact with ***Ia*** and ***IIa***, and we assume that the isatinphenylsemicarbazone associated form A, the non-associated hydrazide form B and the hydrazonol form C are all present in solution at both concentrations. Similar Φ_{E-Z} values for ***Ia*** and ***IIa*** in these solvents indicate similar associate/hydrazide/hydrazonol ratio for these *E*-isomers in solution. Because the Φ_{E-Z} values in MeOH and DMF vary with initial ***Ia*** and ***IIa*** concentration, forms A, B, C should differ in Φ_{E-Z}.

As previously mentioned, decreased *E*-isomer concentration shifts the tautomeric hydrazide-hydrazonol equilibrium in the strongly interacting DMF and MeOH polar solvents to the right, resulting in hydrazonol formation. The increase in Φ_{E-Z} for both *E*-isomers with increasing isatinphenylsemicarbazone concentration in highly interacting polar solvents thus clearly excludes the dominant contribution of hydrazonol form C to *E–Z* isomerization in these solvents. In contrast, the hydrazonol excited state is deactivated through competitive deactivation pathways and hydrazonol C excitation decreases *E–Z* isomerization efficiency by hydrazonol absorption of photochemically active light. Therefore, ***Ia*** and ***IIa*** *Z*-isomers originate from phototransformation of the associated form A and/or hydrazide form B. Although the increase in Φ_{E-Z} with increasing isatinphenylsemicarbazone concentration in strongly interacting polar solvents may be expressly the consequence of hydrazonol C reduction in solution, and *Z*-isomers could thus originate from phototransformation of hydrazide B rather than the

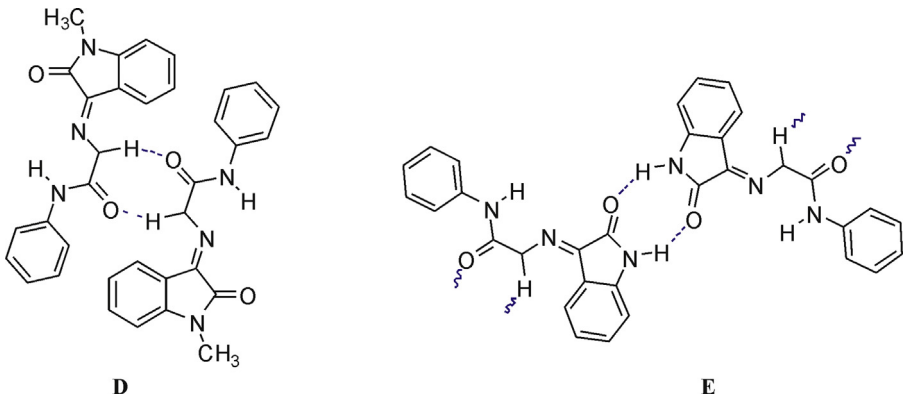

Scheme 3. Assumed aggregation type difference for studied ***IIa*** and ***Ia*** *E*-isomers.

self-aggregate A, we consider that the *Z*-isomers are produced by both excited A and B forms. This conclusion is supported by the Φ_{E-Z} values for ***Ia*** and ***IIa*** in weakly interacting solvents such as benzene, CH_2Cl_2 and MeCN. Despite hydrazonol C absence in these solvents, Φ_{E-Z} again increases with increasing isatinphenylsemicarbazone concentration. Compared to strongly interacting polar solvents, a higher amount of aggregates is present in solution at low isatinphenylsemicarbazone concentrations. Therefore lower Φ_{E-Z} for ***Ia***, and particularly for ***IIa***, in weakly interacting solvents is most likely the consequence of improved *Z*-isomer excited state stabilization in strongly interacting polar solvents which decreases the rate of back *Z*-isomer → aggregate A and/or *Z*-isomer → hydrazide B reaction in their excited states. The increasing *E–Z* isomerization rate after sensitization with benzophenone in MeOH indicates the important role of intersystem crossing in the *E–Z* isomerization mechanism (triplet state generation in the excited hydrazide molecule – Fig. S4).

Although *E*-isomers ***Ia*** and ***IIa*** form associates in both strongly and weakly interacting solvents, the methyl substituent in position 1– of isatin cycle ***IIa*** limits hydrazide associate variation in solution. The methyl derivative ***IIa*** with its cyclic hydrogen bonding most commonly forms the type D dimers (Scheme 3). These dimers can be formed from the ***IIa*** molecule in varying conformational arrangements.

In contrast to ***IIa***, the ***Ia*** *E*-isomer can form several types of aggregates with a large number of bound ***Ia*** molecules in the associate (Scheme 3 – form E). In this case, both the urea NH–CO–NH fragment and also the isatine NH fragment may be involved in the formation of the cyclic associate form. This explanation is consistent with the concentration dependent change in the ***Ia*** *E*-isomer's UV–vis spectrum shape compared to the almost concentration-independent shape for ***IIa*** (Fig. S5). It is considered that the apparently higher Φ_{E-Z} for ***Ia*** than for ***IIa*** in weakly interacting solvents, particularly at higher isatinphenylsemicarbazone concentrations, is associated with this aggregation difference in the two *E*-isomers.

The one order of magnitude lower Φ_{E-Z} for ***IIa*** in benzene compared to Φ_{E-Z} for ***Ia*** at low isatinphenylsemicarbazone concentrations may be associated with the π–π interactions between isatin and the benzene ring which are suppressed in ***IIa*** due to a bulk methyl substituent. However, the actual reason for ***Ia*** and ***IIa*** Φ_{E-Z} difference in this aromatic solvent at low concentrations currently remains unidentified.

3.2. Light initiated Z–E isomerization

The excitation of *Z*-isomers ***Ib*** and ***IIb*** at 405 nm did not lead to their conversion to the corresponding *E*-isomers ***Ia*** and ***IIa***. The light initiated back *Z–E* isomerization was not observed even at 341 nm irradiation wavelength; close to where both *Z*-isomers have

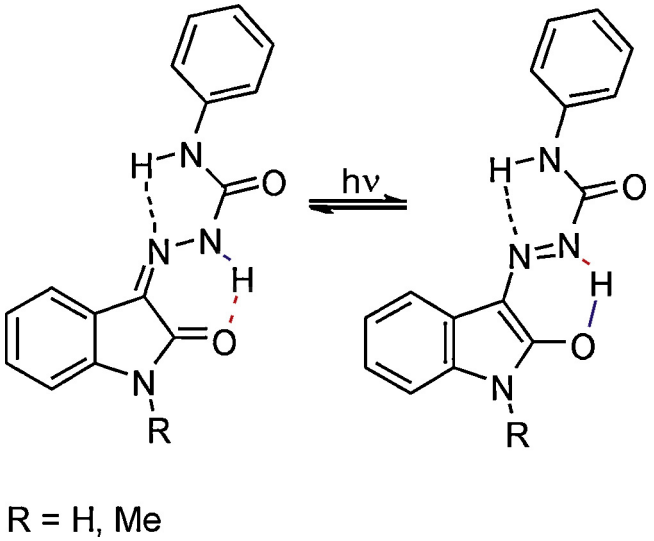

Scheme 4. Assumed excited state proton transfer from strong intramolecular *Z*-isomer hydrogen bonding.

their absorption maxima. Instead of *E*-isomers formation at both irradiation wavelengths, only a very slow photodegradation pathway was observed in weakly interacting polar solvents, no changes were noted under irradiation in the more strongly interacting ones. It is assumed that the absence of back light initiated *Z–E* isomerization results from excited state proton transfer in *Z*-isomer's strong intramolecular hydrogen bonding ([25] and Scheme 4).

The proposed mutual *E–Z* isomer transformations of anion sensors ***I*** and ***II***, including tautomeric equilibrium and aggregate formation, is illustrated in Scheme 5. We assume that the relatively low *E–Z* isomerization efficiency of Φ_{E-Z} <0.01 in all solvents for both ***Ia*** and ***IIa*** *E*-isomers is connected with rapid internal conversion due to the presence of intra- and inter-molecular hydrogen bonding of the hydrazide molecules, and also with the hydrazide–hydrazonol tautomeric equilibrium in strongly interacting polar solvents.

3.3. Thermally initiated E–Z and Z–E isomerization

The study of photochemical *E–Z* isomerization is often complicated by thermally initiated back *Z–E* isomerization. The ratio of individual isomers in the equilibrium is affected by the ratio of the reaction rates running in opposite directions. The potential practical application of *E–Z* isomerization in signal switching, molecular memories and sensors therefore depends on the thermodynamic stability of the less stable isomer. This is typically

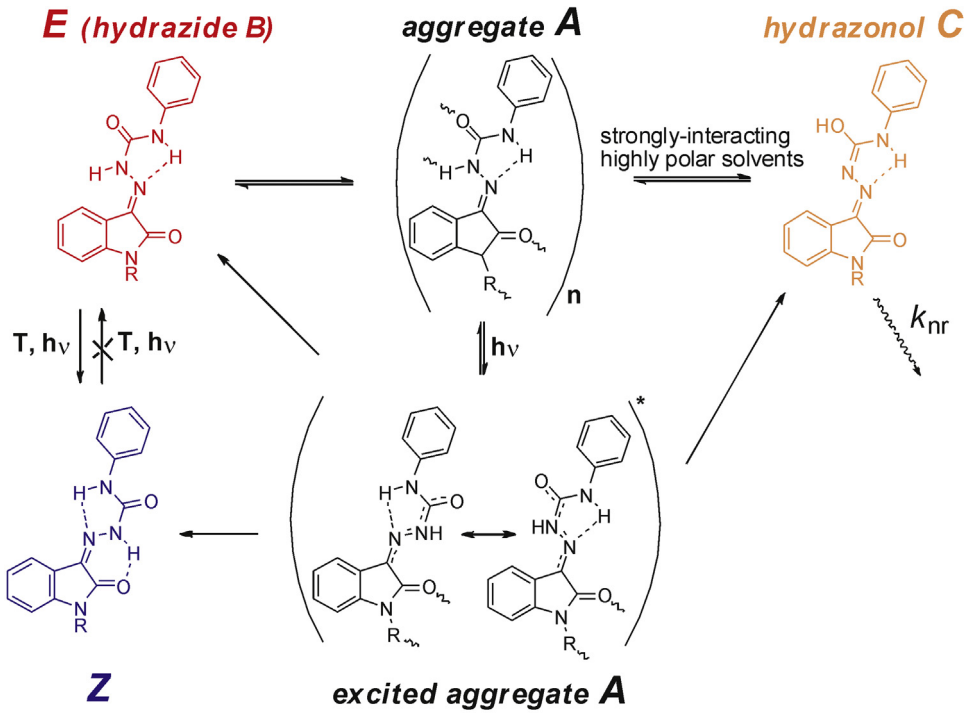

Scheme 5. Mutual *E*–*Z* isomer transformation in the studied ***I*** and ***II*** isatinphenylsemicarbazone anion sensors.

the *Z*-isomer. As mentioned in the Introduction, although *E*–*Z* isomerization of phenylsemicarbazone *E*-isomers ***Ia*** and ***IIa*** occurs in weakly interacting non-polar solvents at room temperature and low isatinphenylsemicarbazone ***Ia*** and ***IIa*** concentrations and in highly interactive polar solvents at temperatures above 70 °C, no formation of the corresponding *E*-isomers was observed during thermally initiated back *Z*–*E* isomerization in any type of solvent [24]. Increased temperature during the ***Ib*** and ***IIb*** solution heating leads only to isatin 3-hydrazone or 1-methylisatin 3-hydrazone decomposition products at both initial ***Ib*** or ***IIb*** concentrations (10^{-6} mol dm^{-3} and 10^{-4} mol dm^{-3}), without formation of the corresponding *E*-isomers (Fig. S6). Therefore, we performed a theoretical study of this problem to show the impossibility of thermal back *Z*–*E* isomerization of ***Ib*** and ***IIb*** in solution.

Fig. 6 graphically illustrates the relative overall energy of *E*- and *Z*-isomers of isatinphenylsemicarbazone ***I*** in conformations ***E1***, ***E2***, ***Z1*** and ***Z2*** (Scheme 6), and the relative energy of the transition states related to the conformational changes in the particular conformer and the geometric change of one isomer to another.

It is concluded from our theoretical calculations that both *E*- and *Z*-isomers in these conformational arrangements have almost planar geometry. ***Z1*** is the most stable conformation of isatinphenylsemicarbazone ***I*** due to the existence of intra-molecular hydrogen bonding between the urea NH hydrogen and the isatine carbonyl oxygen. The ***E1*** and ***Z2*** conformer energy is approximately 20 kJ mol^{-1} higher than that for ***Z1***. The most energetically disfavored is the ***E2*** conformer with its Y-hydrogen arrangement in the urea part of the molecule. The ***E2*** energy is approximately 60 kJ mol^{-1} higher than for conformer ***Z1***. The ***E2*** conformation does not allow intra-molecular hydrogen bond formation. Calculations also showed that the ***E1E2TS*** and ***Z1Z2TS*** energies of the transition states corresponding to the conformational changes are relatively low compared to the energy of the individual conformations. However, the ***E–Z*** and ***Z–E*** isomerization determining steps are the activation energies E_a related to these geometric transformations ($\boldsymbol{E_{a1}}$(***E–Z***) = ***E1Z1TS-E1*** or $\boldsymbol{E_{a2}}$(***E–Z***) = ***E2Z2TS-E2***

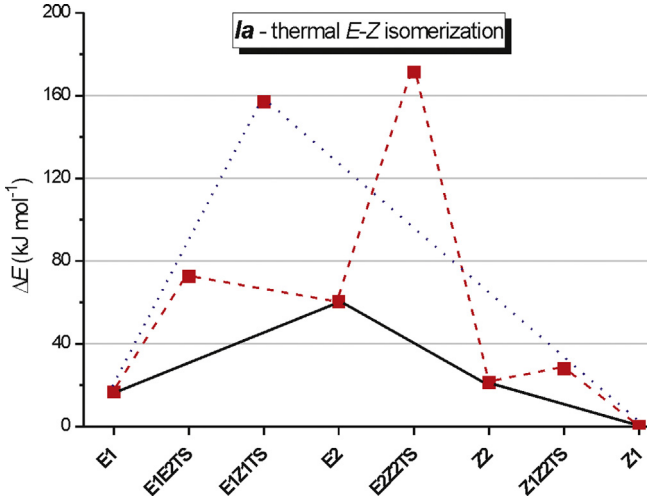

Fig. 6. Calculated relative Gibbs free energies of ***E1***, ***E2***, ***Z1***, ***Z2*** hydrazide conformers of isatinphenylsemicarbazone isomers ***Ia*** and ***Ib*** at the B3LYP 6-31+G(dp)//MP2/6-311++G(d,p) level (T = 298.15 K; TS – transition state).

and $\boldsymbol{E_{a1}}$(***Z–E***) = ***E1Z1TS-Z1*** or $\boldsymbol{E_{a2}}$(***Z–E***) = ***E2Z2TS-Z2***). Gibbs activation energies of the *E*–*Z* and back *Z*–*E* isomerization for the most stable conformers ***E1*** and ***Z1*** are relatively large; and quite similar at $\boldsymbol{E_{a1}}$(***E–Z***) ~ 140 kJ mol^{-1} and $\boldsymbol{E_{a1}}$(***Z–E***) ~ 160 kJ mol^{-1}. Based only on the comparison of these two E_a values, it is impossible to explain the observed ***Ia*** *E*–*Z* isomerization and the absence of back thermally initiated *Z*–*E* isomerization during heating of the *Z*-isomer ***Ib*** solution. The evident difference in reactivity of ***Ia*** and ***Ib*** can be explained by the two-step mechanism of *E*–*Z* isomerization. In the first step, the *E*-isomer conformer ***E2*** is generated through the ***E1E2TS*** transition state. Here, attainment of the equilibrium state between ***E1*** and ***E2*** conformers is temperature dependent. In the second step, *Z*-isomer ***Z1*** and ***Z2***

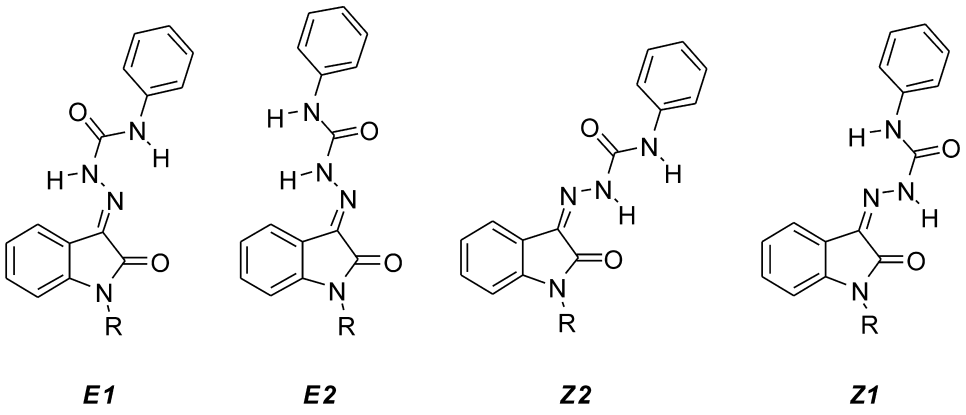

Scheme 6. Hydrazide conformers ***E1***, ***E2***, ***Z1*** and ***Z2*** of the studied isatinphenylsemicarbazone *E*- and *Z*-isomers.

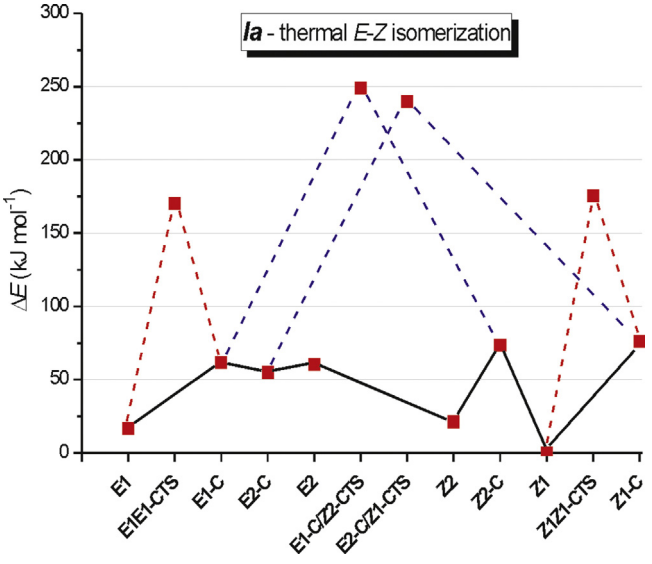

Fig. 7. Calculated relative Gibbs free energies of ***E1***, ***E2***, ***Z1***, ***Z2*** hydrazide and ***E1 – C***, ***E2 – C***, ***Z1 – C***, ***Z2 – C*** hydrazonol conformers of isatinphenylsemicarbazone isomers ***Ia*** and ***Ib*** at the B3LYP 6-31+G(dp)//MP2/6-311++G(d,p) level (T = 298.15 K; TS – transition state).

conformers are formed from the ***E2*** conformer via the ***E2Z2TS*** transition state. The high E_{a1}(***E–Z***) activation energy of 140 kJ mol^{-1} related to *E–Z* isomerization between the most stable conformers ***E1*** and ***Z1*** is counteracted in the two easier energy steps. The ***E2*** formation from ***E1*** consumes 44 kJ mol^{-1} (through activation barrier E_a(***E1–E2***) = ***E1E2TS-E1*** = 53 kJ mol^{-1}), thus reducing the E_{a2}(***E–Z***) = ***E2Z2TS-E2*** barrier for subsequent *E–Z* isomerization to 111 kJ mol^{-1}.

If we assume the same reaction pathway for the back *Z–E* isomerization, the *Z*-isomer conformer ***Z2*** can be easily generated through the transition state ***Z1Z2TS*** (activation energy E_a(***Z1–Z2***) = 25 kJ mol^{-1}). However, in the second step, it is necessary to overcome the high activation barrier E_{a2}(***Z–E***) = ***E2Z2TS-Z2*** of 150 kJ mol^{-1}. This activation energy for *Z–E* isomerization, similar to the activation barrier E_{a1}(***Z–E***) = ***E1Z1TS-Z1*** of 157 kJ mol^{-1}, is so large that that degradation of the *Z*-isomer occurs rather than *E*-isomer formation. This is reflected in experimental results.

In addition to hydrazide B ***E1*** and ***E2*** conformers, hydrazonol form C can also contribute to overall *Z*-isomer formation in strongly interacting polar solvents such as MeOH, DMF and DMSO. Fig. 7 shows the calculated relative overall energy of the corresponding ***E1-C***, ***E2-C***, ***Z1-C*** and ***Z2-C*** hydrazonol C conformers of the isatinphenylsemicarbazone ***I*** *E*- and *Z*-isomers (Scheme 7), and the relative energy of the transition states relating to the conformational changes of the particular hydrazide conformer to the hydrazonol conformer and the geometric change of one hydrazonol isomer to another; together with the relative overall energy of the ***E1***, ***E2***, ***Z1*** and ***Z2*** hydrazide B conformers.

The overall stabilities of the individual ***E1-C***, ***E2-C***, ***Z1-C*** and ***Z2-C*** hydrazonol C conformers are very similar, with energy differences lying within 22 kJ mol^{-1}. Since the formation of the ***E1-C*** hydrazonol form from the ***E1*** hydrazide B form must overcome the surprisingly high activation barrier of approximately 150 kJ mol^{-1} (through ***E1E1-CTS*** transition state), it is very unlikely that hydrazonol ***E1-C*** is formed by this transformation pathway. Experimental results also indicate a different ***E1-C*** formation pathway: hydrazonol form C (***E1-C*** or ***E2-C***) exists in strongly interacting polar solvents at room temperature in equilibrium with the hydrazide form (***E1*** or ***E2***) and almost instantaneous settling of the new equilibrium with higher contents of the hydrazonol C form can result only from dilution of the solution. This rapid equilibrium settlement after dilution indicates that the hydrazide B form of *E*-isomer ***Ia*** exists in solution at higher isatinphenylsemicarbazone ***Ia*** concentration also in the associated A form. The intermolecular hydrogen bonds in the associates create appropriate conditions for hydrogen transfer, and thus also for the formation of the ***E1-C*** hydrazonol C conformer with a significantly lower activation barrier to overcome the ***E1E1-CTS*** transition state energy. Despite ***E1-C*** or ***E2-C*** hydrazonol C form presence in strongly interacting polar solvents at room temperature, the very high subsequent *E–Z* isomerization activation barriers of 185 kJ mol^{-1} for E_{a1}(***E–Z***) = (***E2-C/Z1-CTS***)-(***E2-C***) and 187 kJ mol^{-1} for E_{a2}(***E–Z***) = (***E1-C/Z2-CTS***)-(***E1-C***) exclude hydrazonol C contribution to the thermal ***Ia*** *E–Z* isomerization.

UV–vis spectra of the ***Ib*** and ***IIb*** *Z*-isomers exclude the presence of their hydrazonol C forms in strongly interacting polar solvents. These results concur with the calculated E_a = (***Z1Z1-CTS***)-***Z1*** activation energy above 170 kJ mol^{-1} for the corresponding conformational change from the ***Z1*** hydrazide to the ***Z1-C*** hydrazonol conformer. In contrast to *E*-isomers ***Ia*** and ***IIa***, isatinphenylsemicarbazone *Z*-isomers ***Ib*** and ***IIb*** do not form aggregates in solution and thus the high activation energy for conformational change from hydrazide to hydrazonol conformer remains unchanged even at high *Z*-isomer concentration. The absence of back thermal *Z–E* isomerization of ***Ib*** and ***IIb*** support these conclusions.

Since ***Ib*** and ***IIb*** methylated isomer behavior was very similar to that of the ***Ia*** and ***IIa*** unmethylated isomers in all thermal experiments, we assume that the quantum-chemical calculation conclusions for ***Ia*** and ***IIa*** are also valid for the ***Ib*** and ***IIb*** unmethylated isomers.

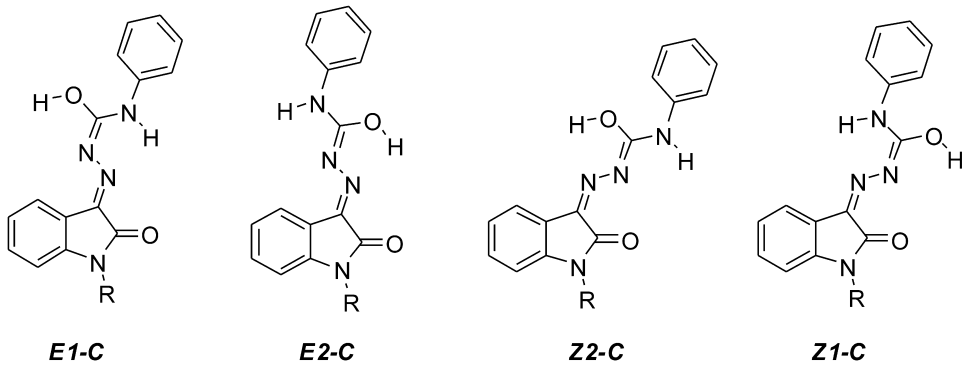

Scheme 7. Hydrazonol conformers ***E*1-C**, ***E*2-C**, ***Z*1-C** and ***Z*2-C** of the studied isatinphenylsemicarbazone *E*- and *Z*-isomers.

4. Conclusion

This paper investigated light and thermally initiated *E*–*Z* and *Z*–*E* isomerization of two efficient isatin *N*-phenylsemicarbazone colorimetric sensors for strongly basic anions in different polarity solvents.

The *E*–*Z* isomerization quantum yield (Φ_{E-Z}) depends on solvent type, *E*-isomer concentration and presence or absence of the $-CH_3$ substituent in position 1 of the isatin skeleton. The increase in Φ_{E-Z} for both *E*-isomers with increasing isatinphenylsemicarbazone concentration in highly interacting polar solvents excludes dominant contribution of hydrazonol form C to the light initiated *E*–*Z* isomerization. In these solvents, the *Z*-isomers are produced by both the excited associated A and the excited hydrazide B forms. Despite hydrazonol C absence in weakly interacting solvents such as benzene, CH_2Cl_2 and MeCN, the Φ_{E-Z} again increases with increasing isatinphenylsemicarbazone concentration and this indicates the aggregated A form's higher contribution to overall *Z*-isomer production. We assume that the relatively low *E*–*Z* isomerization efficiency of $\Phi_{E-Z} < 0.01$ in both solvent types is connected with rapid internal conversion due to the hydrazide molecule's intra- and inter-molecular hydrogen bonds, and also linked to the hydrazide–hydrazonol tautomeric equilibrium in strongly interacting polar solvents. The lower Φ_{E-Z} in weakly interacting solvents compared to that in strongly interacting polar solvents is most likely the consequence of increased *Z*-isomer excited-state stabilization in strongly interacting polar solvents which decreases the rate of back *Z*-isomer → aggregate A and/or *Z*-isomer → hydrazide B reaction in their excited states. The apparently higher Φ_{E-Z} for ***Ia*** than for ***IIa*** in weakly interacting solvents is associated with aggregation type differences in the studied ***Ia*** and ***IIa*** *E*-isomers.

The excitation of *Z*-isomers did not lead to their conversion to the corresponding ***Ia*** and ***IIa*** *E*-isomers. We assume that the absence of back light initiated *Z*–*E* isomerization is the consequence of excited state proton transfer resulting from strong *Z*-isomer intramolecular hydrogen bonding.

We performed a theoretical study to explain the mechanism of thermally initiated *E*–*Z* isomerization at higher temperatures and the impossibility of thermal back *Z*–*E* isomerization of ***Ib*** and ***IIb*** in solution. Our calculations indicated the high activation energy required for back thermal *Z*–*E* isomerization and also the relatively high activation energy required for thermally initiated *E*–*Z* isomerization was decreased in two less energetically demanding steps. Conclusions drawn from these theoretical calculations concurred with our experimental results.

The photodegradation of *E*-isomer anion sensors ***Ia*** and ***IIa*** due to light initiated *E*–*Z* isomerization may complicate the anion detection, therefore care should be taken when interpreting data for quantitative determination of anions using ***Ia*** and ***IIa*** *E*-isomers because of lower *Z*-isomer sensitivity. However, the photochemical *E*–*Z* isomerization efficiency is relatively low at $\Phi_{E-Z} < 0.01$, and this allows reliable detection of strongly basic anions using ***Ia*** or ***IIa***. In addition, the easy *E*-isomer transformation to the corresponding *Z*-isomer and the utilization of both isomers significantly enlarges the detection range for F^- or CH_3COO^- anions valid for ***Ia*** or ***IIa*** in organic media from 0.1–1 equiv. to 0.1–100 equiv. of isatinphenylsemicarbazone (from 10^{-5} mol dm^{-3} to 10^{-2} mol dm^{-3} of F^- or CH_3COO^-) without interference at high excess of weak basic anions. Using the different path length, this range can be further enlarged to 10^{-6}–10^{-1} mol dm^{-3}. The detection range is shifted to higher anion concentrations in semi-aqueous media because of water competition.

Although the zero efficiency of back photochemical *Z*–*E* isomerization excludes the use of isatinphenylsemicarbazones ***I*** and ***II*** as molecular switches, the absence of thermally initiated *E*–*Z* isomerization and both photochemically and thermally initiated back *Z*–*E* isomerizations in strongly interacting polar solvents can prove beneficial for ***Ia*** and ***IIa*** *E*-isomer application in chemical actinometry.

Acknowledgment

The authors greatly appreciate the financial support provided by the VEGA Grant Agency (Grant No. 1/1126/11).

Appendix A. Supplementary data

Supplementary material related to this article can be found, in the online version, at http://dx.doi.org/10.1016/j.jphotochem.2014.05.004.

References

[1] H. Durr, General introduction, in: H. Durr, H. Bouas-Laurent (Eds.), Photochromism: Molecules and Systems, Elsevier Science Publishers B.V., Amsterdam, 1990, pp. 1–14.
[2] M. Irie, Photochromism: memories and switchess—introduction, Chem. Rev. 100 (2000) 1683–1684, http://dx.doi.org/10.1021/cr980068l.
[3] G. Berkovic, V. Krongaus, V. Welss, Spiropyrans and spirooxazines for memories and switches, Chem. Rev. 100 (2000) 1741–1753, http://dx.doi.org/10.1021/cr9800715.
[4] W. Yuan, L. Sun, H. Tang, Y. Wen, G. Jiang, W. Huang, L. Jiang, Y. Song, H. Tian, D. Zhu, A novel thermally stable spironaphthoxazine and its application in rewritable high density optical data storage, Adv. Mater. 17 (2005) 156–160, http://dx.doi.org/10.1002/adma.200400953.
[5] R. Klajn, Spiropyran-based dynamic materials, Chem. Soc. Rev. 43 (2014) 148–184, http://dx.doi.org/10.1039/c3cs60181a.
[6] G. Vantomme, J.M. Lehn, Photo- and thermoresponsive supramolecular assemblies: reversible photorelease of K^+ ions and constitutional dynamics, Angew. Chem. Int. Ed. 52 (2013) 3940–3943, http://dx.doi.org/10.1002/anie.201210334.

[7] X. Su, I. Aprahamian, Hydrazone-based switches, metallo-assemblies and sensors, Chem. Soc. Rev. (2014), http://dx.doi.org/10.1039/c3cs60385g.
[8] J.S. Wu, W.M. Liu, X.Q. Zhuang, F. Wang, P.F. Wang, S.L. Tao, X.H. Zhang, S.K. Wu, S.T. Lee, Fluorescence turn on of coumarin derivatives by metal cations: a new signaling mechanism based on C=N isomerization, Org. Lett. 9 (2007) 33–36, http://dx.doi.org/10.1021/ol062518z.
[9] P.F. Wang, S.K. Wu, Spectroscopy and photophysics of bridged enone derivatives: effect of molecular structure and solvent, J. Photochem. Photobiol. A 86 (1995) 109–113.
[10] I. Karube, Y. Nakamoto, K. Namba, S. Suzuki, Photocontrol of urease-collagen membrane activity, Biochim. Biophys. Acta 429 (1976) 975–981.
[11] I. Rubinstein, A.J. Bard, Unique properties of chromophore-containing bilayer aggregates: enhanced chirality and photochemically induced morphological change, J. Am. Chem. Soc. 102 (1980) 6641–6642, http://dx.doi.org/10.1021/ja00541a080.
[12] S. Shinkai, T. Nakaji, T. Ogawa, K. Shigematsu, O. Manabe, Photoresponsive crown ethers. 2. Photocontrol of ion extraction and ion transport by a bis(crown ether) with a butterfly-like motion, J. Am. Chem. Soc. 103 (1981) 111–115, http://dx.doi.org/10.1021/ja00391a021.
[13] P.J. Smith, M.V. Reddington, C.S. Wilcox, Ion pair binding by a urea in chloroform solution, Tetrahedron Lett. 33 (1992) 6085–6088, http://dx.doi.org/10.1016/S0040-4039(00)60012-6.
[14] E. Fan, S.A. van Arman, S. Kincaid, A.D. Hamilton, Molecular recognition: hydrogen-bonding receptors that function in highly competitive solvents, J. Am. Chem. Soc. 115 (1993) 369–370, http://dx.doi.org/10.1021/ja00054a066.
[15] T. Steiner, The hydrogen bond in the solid state, Angew. Chem. Int. Ed. 41 (2002) 48–76, http://dx.doi.org/10.1002/1521-3773(20020104)41:1<48::AID-ANIE48>3.0.CO;2-U.
[16] M. Boiocchi, L.D. Boca, D.E. Gómez, L. Fabbrizzi, L. Licchelli, E. Monzani, Nature of urea–fluoride interaction: incipient and definitive proton transfer, J. Am. Chem. Soc. 126 (2004) 16507–16514, http://dx.doi.org/10.1021/ja045936c.
[17] M. Wenzel, M.E. Light, A.P. Davis, P.A. Gale, Thiourea isosteres as anion receptors and transmembrane transporters, Chem. Commun. 47 (2011) 7641–7643, http://dx.doi.org/10.1039/C1CC12439K.
[18] M.G. Chudzinski, C.A. Corey, A. McClary, M.S. Taylor, Anion receptors composed of hydrogen- and halogen-bond donor groups: modulating selectivity with combinations of distinct noncovalent interactions, J. Am. Chem. Soc. 133 (2011) 10559–10567, http://dx.doi.org/10.1021/ja20 2096.
[19] G. Bergamaschi, M. Boiocchi, E. Monzani, V. Amendola, Pyridinium/urea-based anion receptor: methine formation in the presence of basic anions, Org. Biomol. Chem. 9 (2011) 8276–8283, http://dx.doi.org/10.1039/C1OB06193C.
[20] M.B. Jiménez, V. Alcázar, R. Paláez, F. Sanz, A.L. Fuentes de Arriba, M.C. Caballero, Bis-amidocarbazolyl urea receptor for short-chain dicarboxylate anions, Org. Biomol. Chem. 10 (2012) 1181–1185, http://dx.doi.org/10.1039/C1OB06540H.
[21] L.E. Santos-Figueroa, M.E. Moragues, E. Climent, A. Agostini, R. Martínez-Máñez, F. Sancenón, Chromogenic and fluorogenic chemosensors and reagents for anions. A comprehensive review of the years 2010–2011, Chem. Soc. Rev. 42 (2013) 3489–3613, http://dx.doi.org/10.1039/c3cs60316d.
[22] P.A. Gale, N. Busschaert, C.J.E. Haynes, L.E. Karagiannidis, I.L. Kirby, Anion receptor chemistry: highlights from 2011 and 2012, Chem. Soc. Rev. (2014), http://dx.doi.org/10.1039/c3cs60316d.
[23] K. Jakusová, J. Donovalová, M. Cigáň, M. Gaplovský, V. Garaj, A. Gaplovský, Isatinphenylsemicarbazones as efficient colorimetric sensors for fluoride and acetate anions—anions induce tautomerism, Spectrochim. Acta A 123 (2014) 421–429, http://dx.doi.org/10.1016/j.saa.2013.12.073.
[24] K. Jakusová, J. Donovalová, M. Gaplovský, M. Cigáň, H. Stankovičová, A. Gaplovský, Self association, tautomerism and E–Z isomerization of isatin-phenylsemicarbazones – spectral study and theoretical calculations, J. Phys. Org. Chem. (2013), http://dx.doi.org/10.1002/poc.3164.
[25] K. Jakusová, M. Gáplovský, J. Donovalová, M. Cigáň, H. Stankovičová, R. Sokolík, J. Gašpar, A. Gáplovský, Effect of reactants' concentration on the ratio and yield of E,Z isomers of isatin-3-(4-phenyl)semicarbazone and N-methylisatin-3-(4-phenyl)semicarbazone, Chem. Pap. 67 (2013) 117–126, http://dx.doi.org/10.2478/s11696-012-0248-x.
[26] A. Gáplovský, Š. Toma, J. Donovalová, Reactors for simultaneous application of UV light and ultrasound on the reaction mixture and their modifications for kinetic studies, J. Photochem. Photobiol. A: Chem. 191 (2007) 162–166, http://dx.doi.org/10.1016/j.jphotochem.2007.04.018.
[27] P. Klán, J. Wirz, Spectrophotometric determination of the reaction progress, in: J. Coxon, P. Bailey, L. Field, J.A. Gladysz, P. Parsons, P. Stang (Eds.), Photochemistry of Organic Compounds: From Concepts To Practice, John Wiley & Sons Ltd., Chichester, 2009, pp. 114–116.
[28] E.S. Galbavy, K. Ram, C. Anastasio, 2-Nitrobenzaldehyde as a chemical actinometer for solution and ice photochemistry, J. Photochem. Photobiol. A: Chem. 209 (2010) 186–192, http://dx.doi.org/10.1016/j.jphotochem.2009.11.013.
[29] M.J. Frisch, G.W. Trucks, H.B. Schlegel, G.E. Scuseria, M.A. Robb, J.R. Cheeseman, G. Scalmani, V. Barone, B. Mennucci, G.A. Petersson, H. Nakatsuji, M. Caricato, X. Li, H.P. Hratchian, A.F. Izmaylov, J. Bloino, G. Zheng, J.L. Sonnenberg, M. Hada, M. Ehara, K. Toyota, R. Fukuda, J. Hasegawa, M. Ishida, T. Nakajima, Y. Honda, O. Kitao, H. Nakai, T. Vreven, J.A. Montgomery Jr., J.E. Peralta, F. Ogliaro, M. Bearpark, J.J. Heyd, E. Brothers, K.N. Kudin, V.N. Staroverov, R. Kobayashi, J. Normand, K. Raghavachari, A. Rendell, J.C. Burant, S.S. Iyengar, J. Tomasi, M. Cossi, N. Rega, N.J. Millam, M. Klene, J.E. Knox, J.B. Cross, V. Bakken, C. Adamo, J. Jaramillo, R. Gomperts, R.E. Stratmann, O. Yazyev, A.J. Austin, R. Cammi, C. Pomelli, J.W. Ochterski, R.L. Martin, K. Morokuma, V.G. Zakrzewski, G.A. Voth, P. Salvador, J.J. Dannenberg, S. Dapprich, A.D. Daniels, Ö. Farkas, J.B. Foresman, J.V. Ortiz, J. Cioslowski, D.J. Fox, Gaussian 09, Revision A1, Gaussian Inc., Wallingford, CT, 2009.
[30] V. Gutmann, Empirical parameters for donor and acceptor properties of solvents, Electrochim. Acta 21 (1976) 661–670, http://dx.doi.org/10.1016/0013-4686(76)85034-7.